

TRIGGER EVENTS: ENVIROCLIMATIC COUPLING OF EBOLA HEMORRHAGIC FEVER OUTBREAKS

JORGE E. PINZON, JAMES M. WILSON, COMPTON J. TUCKER, RAY ARTHUR, PETER B. JAHRLING, AND
PIERRE FORMENTY

Biospheric Sciences Branch, Laboratory for Terrestrial Physics, National Aeronautics and Space Administration-Goddard Space Flight Center, Greenbelt, Maryland; Science Systems & Applications, Inc., Lanham, Maryland; Global Alert and Response Team, Department of Communicable Diseases Surveillance and Response, World Health Organization, Geneva, Switzerland; U.S. Army Medical Research Institute for Infectious Disease, Fort Detrick, Frederick, Maryland

Abstract. We use spatially continuous satellite data as a correlate of precipitation within tropical Africa and show that the majority of documented Ebola hemorrhagic fever outbreaks were closely associated with sharply drier conditions at the end of the rainy season. We propose that these trigger events may enhance transmission of Ebola virus from its cryptic reservoir to humans. These findings suggest specific directions to help understand the sylvatic cycle of the virus and may provide early warning tools to detect possible future outbreaks of this enigmatic disease.

INTRODUCTION

Ebola hemorrhagic fever (EHF), which is caused by a virus of the family Filoviridae, affects human and non-human primates and perhaps other animals. Four genetic subtypes of Ebola hemorrhagic fever virus have been reported: Zaire, Côte d'Ivoire, Sudan, and Reston.¹ Ebola hemorrhagic fever was first identified in 1976 when two epidemics occurred almost simultaneously in northwestern Democratic Republic of Congo (formerly Zaire) and southern Sudan.^{2,3} One year after these outbreaks, a patient with Ebola hemorrhagic fever sought treatment at a mission hospital in Tandala, Democratic Republic of Congo.⁴ Another epidemic was identified at the same location in southern Sudan in 1979.⁵

Ebola hemorrhagic fever was not reported again until the end of 1994, when three outbreaks started almost simultaneously. In November 1994, ethnologists studying chimpanzees (*Pan troglodytes verus*) in Tai National Park in Côte d'Ivoire found dead chimpanzees and noticed the absence of others. One dead chimpanzee was found to be infected with Ebola virus, and one researcher was infected with Ebola during a chimpanzee necropsy.^{6,7} The following month, Ebola outbreaks were reported in Gabon and the Democratic Republic of Congo. Multiple human cases were reported in northeastern Gabon in the gold panning camps of Mekouka, Andock, and Minkebe,^{8,9} and a large human Ebola outbreak began in the Kikwit District in the Democratic Republic of Congo.¹⁰ The Kikwit outbreak resembled the 1976 episodes in Yambuku, Democratic Republic of Congo where secondary transmission of the virus in Kikwit occurred through close personal contact in families and hospitals where infection control mechanisms were not in place because of economic constraints. Retrospective case analysis suggests that the index case may have been a charcoal maker that worked in the forest outside Kikwit and was presumably exposed through an unknown mechanism to the virus. In Kikwit, human-to-human transmission occurred without being recognized until the end of April 1995. Additional human outbreaks were reported in February 1996 in Mayibout II, Gabon, a village 40 km south of the original outbreak in the gold panning camps, and in July 1996 at a logging camp between Ovan and Koumameyong, near Booué.⁹

Ape carcasses were found near the sites of three Ebola hemorrhagic fever outbreaks in Gabon; however from 1994 to 1997, only one chimpanzee was found to be Ebola positive in

Lopé Park near Booué in August 1996. Circumstantial reports attribute the February 1996 Gabon outbreak to infection after butchering a dead chimpanzee, although this has not been verified.⁹

The largest Ebola hemorrhagic fever epidemic to date occurred in the Gulu District in Uganda from August 2000 to January 2001.^{11,12} Epidemiologic investigation of this epidemic showed intra-familial and nosocomial transmission similar to the Kikwit outbreak.

From October 2001 to July 2002, several Ebola outbreaks were reported in the Ogooue-Ivindo Province of Gabon and in the Mbomo and Kélé districts in the Republic of the Congo.¹³ In August and September 2001, a die-off of chimpanzees, gorillas, and duikers was reported in Gabon.¹⁴ Then in December 2002, another outbreak of Ebola occurred in humans in Kélé. This outbreak was again preceded by a die-off of chimpanzees, gorillas, and duikers in November 2002 that were laboratory-positive for Ebola infection.¹⁵

Ebola virus affects non-human primates, and recent work suggested a gradual spread of Ebola hemorrhagic fever virus within gorilla and chimpanzee communities in western equatorial Africa with a dramatic decrease noted in population numbers.¹⁶ Non-human primates have been implicated as the source of several, but not all, human outbreaks through contact with infected ape meat acquired through hunting. We consider the possibility that Ebola outbreaks in non-human primates may occur independently of human cases. This raises the potential problem of distinguishing primary Ebola outbreaks from undetected, residual outbreaks that re-emerge from a non-human primate source, usually through the bush meat trade.

Despite extensive field investigations to define the ecology of the virus, the mechanism of transmission from its reservoir to non-human primates and humans remains a mystery. Filoviruses do not persist in experimentally infected non-human primates. Non-human primates are probably not the natural reservoir and, similar to humans, these species are probably infected when direct or indirect contact is made with the natural host. No Ebola viruses or antibodies against Ebola virus were identified in the more than 32,000 animals including arthropods, mammals, avians, and reptiles tested at several sites in Africa as potential candidate reservoir species.^{12–15,17–21}

Multiple factors likely contribute to the appearance of Ebola hemorrhagic fever in non-human primates and hu-

mans. Of interest is the spatial specificity, seasonal context, and occasional temporal clustering of Ebola hemorrhagic fever outbreaks. Ebola epidemics in Nzara, Sudan and Yambuku, Democratic Republic of Congo in 1976 occurred within two months of each other in two geographic locations separated by hundreds of kilometers involving two separate viral strains (Sudan and Zaire). The outbreaks of Tai, Côte d'Ivoire, Mekouka, Gabon, and Kikwit, Democratic Republic of Congo in late 1994 also occurred within two months of each other in three different geographic regions involving two viral strains (Côte d'Ivoire and Zaire). Fifteen years passed between the 1976–1979 and 1994–1996 temporal clusters of Ebola cases without identification of additional outbreaks in equatorial Africa. The late 2000 Uganda outbreak and the late 2001 Gabon outbreaks occurred seven and eight years after the 1994 outbreaks.

Prior studies have suggested possible enviroclimatic influence of Ebola fever incidence due to the predominant appearance of epidemics at the end of the rainy season and/or the start of the dry season.^{6,22,23} Tucker and others analyzed Landsat data from all reported Ebola outbreak locations and found either gallery tropical forest or continuous tropical forest at every outbreak location, in addition to a significant negative climatological anomaly associated with the 1994 cluster of outbreaks.²⁴ These initial studies suggest Ebola virus emerges from its cryptic reservoir in a specific geotemporal and enviroclimatic context. While we acknowledge the multi-factorial nature of epidemic triggering and propagation, these studies implied an ongoing need to evaluate remotely sensed data for use in predictive disease risk modeling, otherwise known as Remotely Sensed Epidemic Surveillance.²⁵ Here we investigate the possibility that enviroclimatic trigger events preceded all initial Ebola outbreaks from 1994 to 2002, using time series satellite data from July 1981 to the present.

MATERIALS AND METHODS

Epidemiologic data. Ebola hemorrhagic fever epidemics were identified on the basis of previously documented, clinically described, and laboratory-confirmed cases (Table 1). When available, the date of symptom onset was noted for the index case (either human or non-human primate) of each outbreak or isolated case. We are possibly introducing errors into the analysis because initial Ebola infection has been documented within ape populations with occasional subsequent human infection such as the 1994 Tai National Park Ebola outbreak.^{6,7,13–16}

Remotely sensed data. An 8 × 8 km grid cell with bi-monthly Normalized Difference Vegetation Index (NDVI) time series data is used as a proxy indicator of enviroclimatic conditions that we associate with Ebola outbreaks. The NDVI data were derived from the Advanced Very High Resolution Radiometer (AVHRR) instrument carried on polar orbiting National Oceanic and Atmospheric Administration (NASA) series of meteorologic satellites and processed by the Global Inventory Modeling and Mapping Studies group at the NASA Goddard Space Flight Center.^{26–30} The NDVI is computed from the upper green and red (550–700 nm) and near infrared (730–1100 nm) channels of the AVHRR instrument as $NDVI = (near\ infrared - red) / (near\ infrared + red)$.

High values of NDVI (~+0.6) are representative of dense green canopies with a high concentration of chlorophyll, while low values (~-0.1) are indicative of sparse vegetation cover and stressed vegetation.^{31,32} The NDVI data provide a temporally and spatially consistent inventory of global gridded time series at 8 km resolution using bi-monthly maximum composites.^{28–33}

A number of studies have shown that NDVI time series are a surrogate for vegetation response to rainfall and evapotranspiration in a wide range of environmental conditions. The NDVI is a surrogate for photosynthetic capacity since it is highly correlated to the absorbed fraction of photosynthetically active radiation (FPAR) and thus gross photosynthesis.³³ We use the NDVI to infer the FPAR, which is directly influenced by rainfall. The NDVI time series has been used to investigate ecologic dynamics and enviroclimatically coupled diseases.^{34–38}

The documented Ebola hemorrhagic fever outbreaks that occurred within the 1981–2003 satellite record were located by the closest geographic coordinates and their respective NDVI were extracted. The mean value, variance, and seasonal profiles of NDVI were used to identify regions (8 × 8 km grid points) of continental Africa with similar characteristics to those from the Ebola sites.

Figure 1 shows the NDVI seasonal patterns for the sites of reported Ebola outbreaks within the satellite record and the NDVI time series during that period. These signals present a characteristic bimodal/unimodal rainy season pattern proper of tropical forest and tropical gallery forest within a savanna matrix of equatorial Africa. Of interest is the unique unimodal seasonal context of the Democratic Republic of Congo and Uganda Ebola incidences compared with the bimodal rainy season patterns from the Gabon, Congo and Côte d'Ivoire signals. The Nzara, Sudan site was added for com-

TABLE 1
Epidemic locations and date of exposure of the index case or first documented case at each location*

| Epidemic site | Ebola subtype | Date of index case clinical presentation | Cases/deaths |
|--|---------------------|--|--------------|
| Tai, Côte d'Ivoire | Ebola Côte d'Ivoire | Oct 1994 | 12(1)/12 (0) |
| Mekouka, Andock, Minkebe, Gabon | Ebola-Zaire | Nov 1994 | 49/29 |
| Kikwit, DRC | Ebola-Zaire | Dec 1994 | 315/242 |
| Mayibout II, Gabon | Ebola-Zaire | Jan 1996 | 31/21 |
| Booue, Gabon | Ebola-Zaire | Jul 1996 | 60/40 |
| Gulu, Uganda | Ebola-Sudan | Sep 2000 | 425/224 |
| Mékambo, Gabon to Kelle and Mbomo, Congo | Ebola-Zaire | Oct 2001 | 124/97 |
| Kelle and Mbomo, Congo | Ebola-Zaire | Dec 2002 | 143/128 |

* Chimpanzee cases are noted at the Tai site with the human exposure noted in parentheses. DRC = Democratic Republic of the Congo.

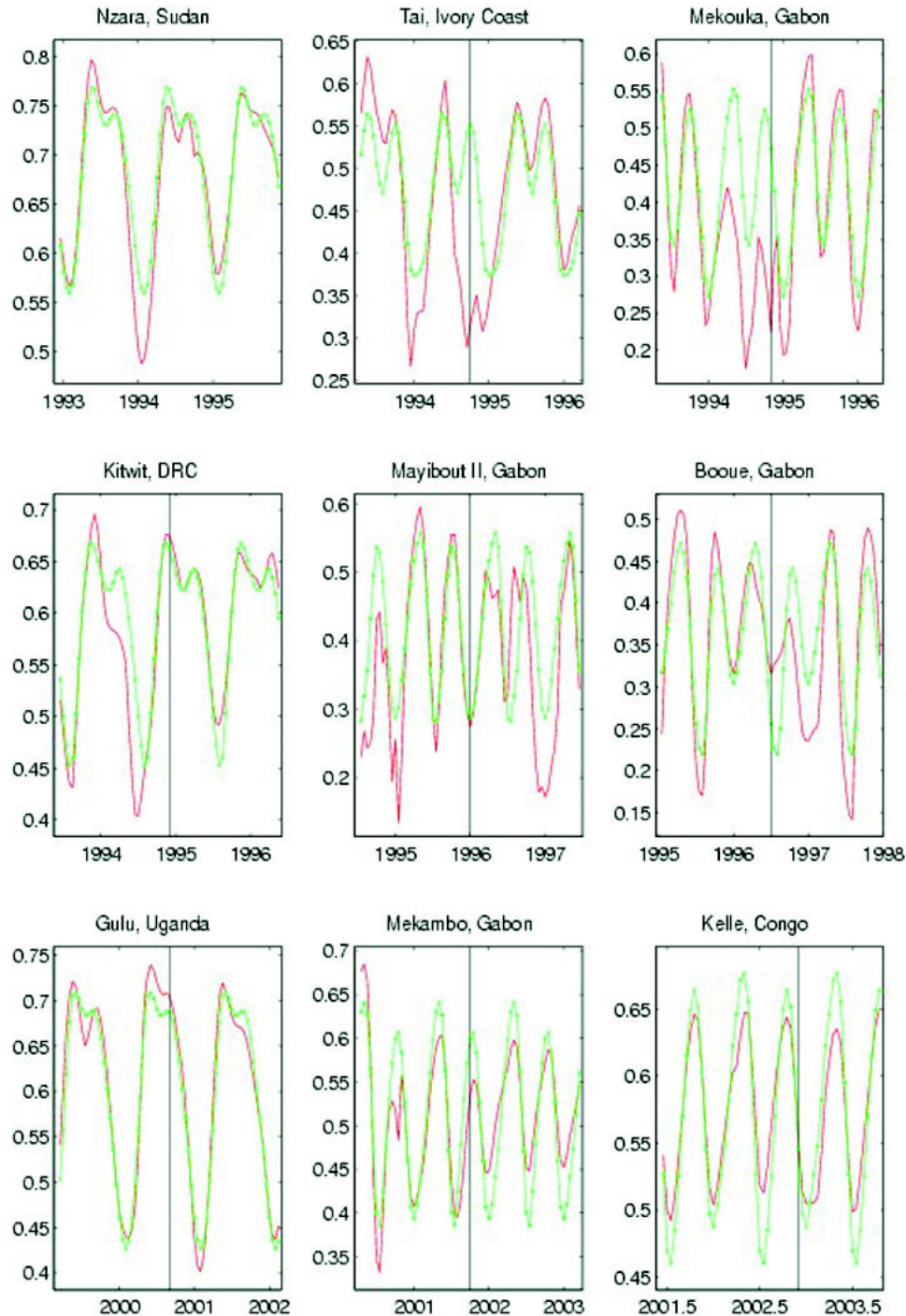


FIGURE 1. Bimonthly Normalized Difference Vegetation Index (NDVI) seasonal average of each reported Ebola incidence (**dotted light line**) versus the NDVI signal of the area during the months before and after the appearance of Ebola (**dark line**). The bisecting **vertical line** indicates the first reported appearance of Ebola for the given site, except for the figure for Nzara, which draws comparison between Nzara and Kikwit due to noted environmental similarities between the two sites. The first column shows the areas with a unimodal rainy season. All of the other outbreak sites display a bimodal rainy season. DRC = Democratic Republic of Congo. This figure appears in color at www.ajtmh.org.

parison with the Democratic Republic of Congo and Uganda sites because of noted similarities in the unimodal seasonal behavior; however, cases of Ebola were not documented in Sudan within the time period of the satellite record analyzed. The bimodal signals show a large deficit of the NDVI with respect to the seasonal pattern (negative anomaly) during the months prior to first appearance of the virus. The Kéllé, Re-

public of Congo NDVI time series does not show this negative anomaly; however, the Mekambo, Gabon time series does, which supports the observation that the cases in Kéllé, Republic of Congo represented an extension of the Mekambo, Gabon outbreak. Note also that a negative NDVI anomaly was found at the Kikwit site during the first months of 1994, but was not associated with the immediate outbreak.

A major drought was observed in 1994 in the immediate areas of the bimodal signals (i.e., the Côte d'Ivoire and Gabon sites) but not the unimodal sites (i.e., the Democratic Republic of Congo and Uganda sites).

Figure 2 shows half geographic degree boxes around the reported Ebola sites; regions with similar spatial and temporal characteristics color-coded by site; and regions with seasonal correlation higher than 0.85, which may indicate risk of Ebola transmission. The regions shown in Figure 2b are stratified according to type of rainy season (bimodal or unimodal). Figure 2c shows the first evidence of enviroclimatic coupling. The results in Figure 2d were estimated from 538 composites (i.e., 24 per year, July 1981 to October 2003) and were tested at a 95% confidence level ($r \geq 0.92$) using a two-tailed *t*-test. High spatial coherence was found among the pixels at this confidence level, i.e., the distance to Ebola outbreaks were less than 220 km or 2 degrees.

To extract features that indicate the possibility of enviroclimatic trigger events during Ebola outbreaks a Canonical Correlation Analysis (CCA) for each year is performed. The yearly CCA analyses were based on a singular value decom-

position (SVD) of the paired-mode correlation matrix (A) between the 24 composites of NDVI signals from the Ebola sites at the year of outbreak (right field) and the 24 composites corresponding to the year of analysis from the regions correlated to Ebola sites (left field) as presented in Figure 2d.

The SVD is a method of finding linear combinations of unitary matrices U and V such that the individual covariances are maximized. The solution given by an SVD matrix decomposition is $[U, S, V] = \text{SVD}(A)$, where $A = USV'$.

The notation ' means the transpose of a vector or matrix. In this expression, U and V are matrices whose columns are orthonormal (unitary matrices) and S is a diagonal matrix whose diagonal elements are the positive singular values sort in descending order.

The CCA is a multivariate statistical technique used to examine and describe the strength of a linear association between two sets of random variables (left and right fields).³⁹⁻⁴¹ This analysis produces a set of orthonormal vectors for the satellite NDVI signals (U) and Ebola sites (V), which are referred to as the canonical factors and are sorted in descending order in terms of the percentage of the covariance ex-

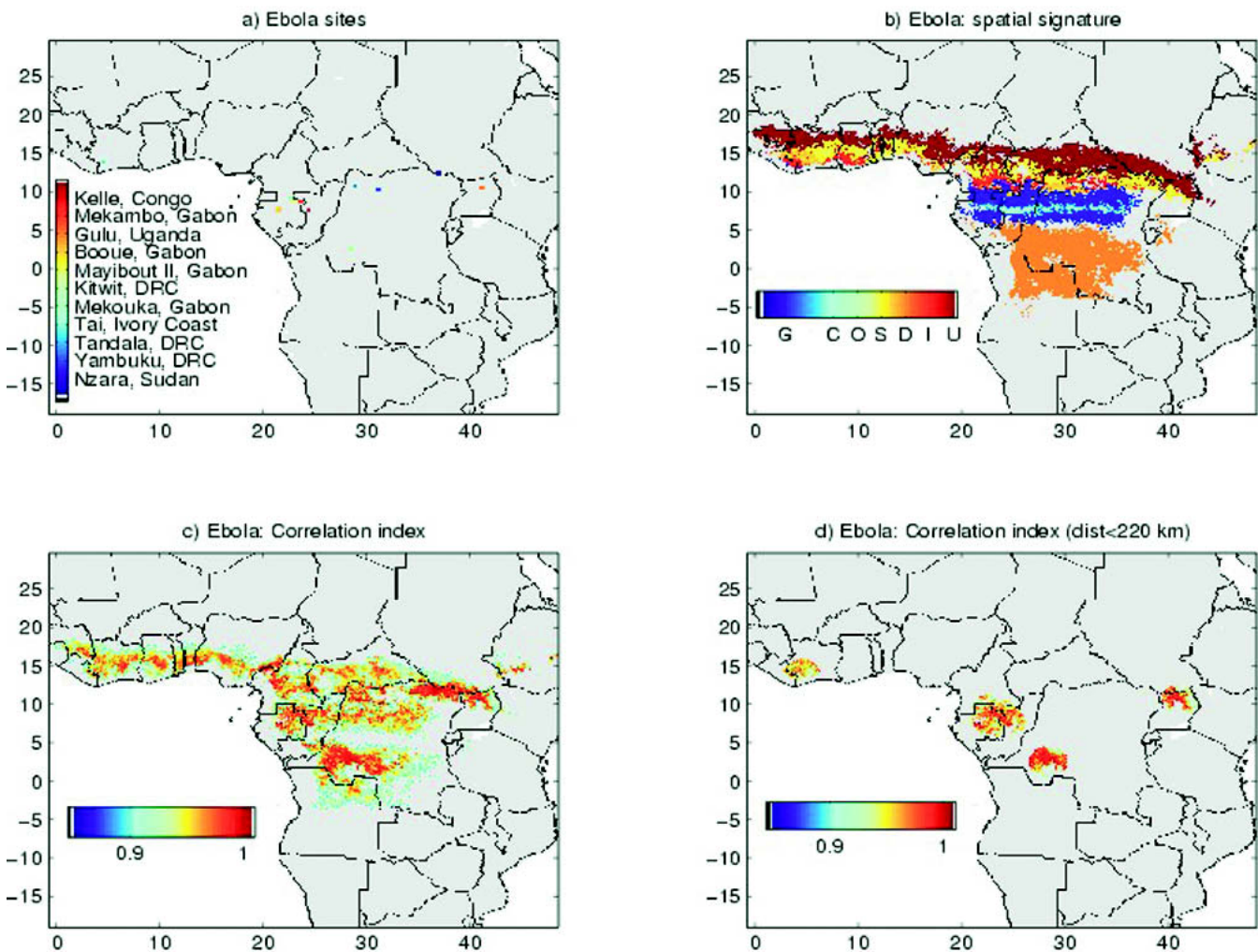


FIGURE 2. Spatial characteristics of Ebola outbreak sites. **a**, Half geographic degree boxes around the reported Ebola sites to denote locations and color coded by site. **b**, Regions with similar spatial and temporal characteristics color-coded by site, **c**, Regions with seasonal correlation higher than 0.85, which may indicate risk of Ebola transmission. **d**, Narrower display of regions in which distances to Ebola incidences are less than two geographic degrees. DRC = Democratic Republic of Congo. This figure appears in color at www.ajtmh.org.

plained by the canonical factors (S). Of great importance is that the leading paired-modes between annual NDVI images and annual NDVI time series of regions of Ebola incidences from the CCA are the largest signal involved between them in both the temporal and spatial domains. In this case, this largest signal can be used to identify for all Africa, regions that can be associated with Ebola incidences through the canonical factor leading modes, and thus develop a temporal-spatial risk index map for Africa.

To focus the analysis on the dominant modes of covariability, we performed CCA using standardized, seasonal-mean leading principal factors.³⁹ Before the results are shown, a few

preliminary comments regarding statistical significance are in order. As in many applications of CCA, we are dealing with fields in which the number of grid points used have a relatively small number of realizations in the time domain. The number of degree of freedom in the correlation coefficients derived from the normalized NDVI data set would be 22 in the absence of year-to-year correlation. In this report, we rely on simple two-tailed *t*-tests performed on 64 Monte Carlo simulations for assessing the statistical significance of the results in which 5% of the grid points were selected randomly. A 5% significance level ($r \geq 0.7$) using a two-tailed *t*-test is reported.

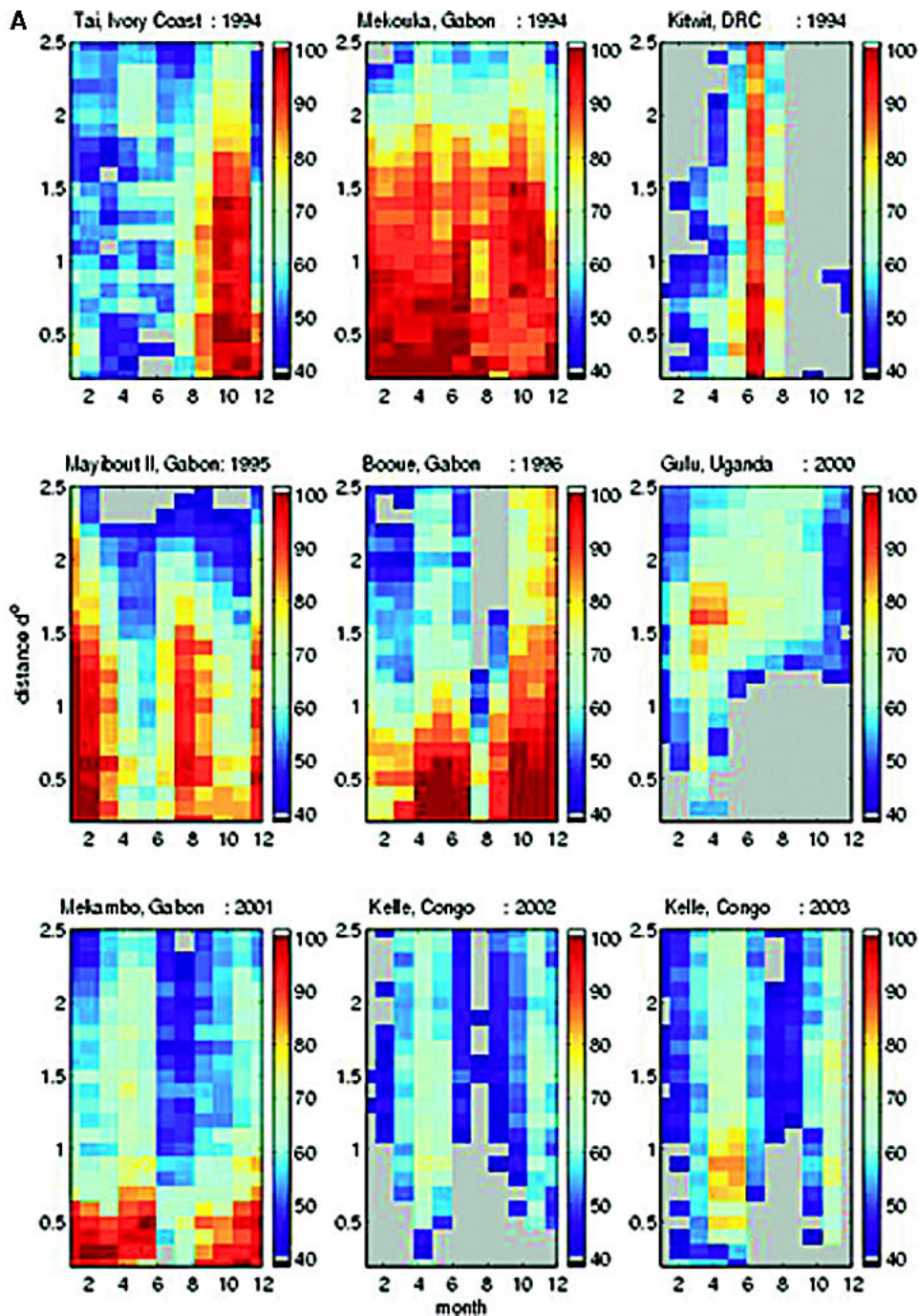


FIGURE 3.

Since the CCA isolates linear combinations of variables that optimize the correlations within two fields, a criterion to determine when a pixel is anomalous can be defined in terms of the integration of the first five canonical vectors for each pixel with a negative anomaly, hereafter called the Ebola Geo-Temporal Trigger (EGT2) index

$$EGT2 = \sum_{j=1}^{Nc} U(:, 1 : Nc)S(1 : Nc, 1 : Nc)V(j, 1 : Nc)'$$

where U, S, and V are the canonical components given by the CCA, Nc represents the five most important components

used in this study, and the notation ' represents the transpose of a vector or matrix. A pixel with an EGT2 index > 0.9 is counted as a pixel involved in each trigger event. For display purposes, this index is normalized by their maximum value (2.5). Adding all EGT2 pixel values for a particular year provides an annual overall Trigger Index (R).

RESULTS

Figure 3A shows the percentage of pixels at 8 km resolution with a negative anomaly near an outbreak site at less than 275

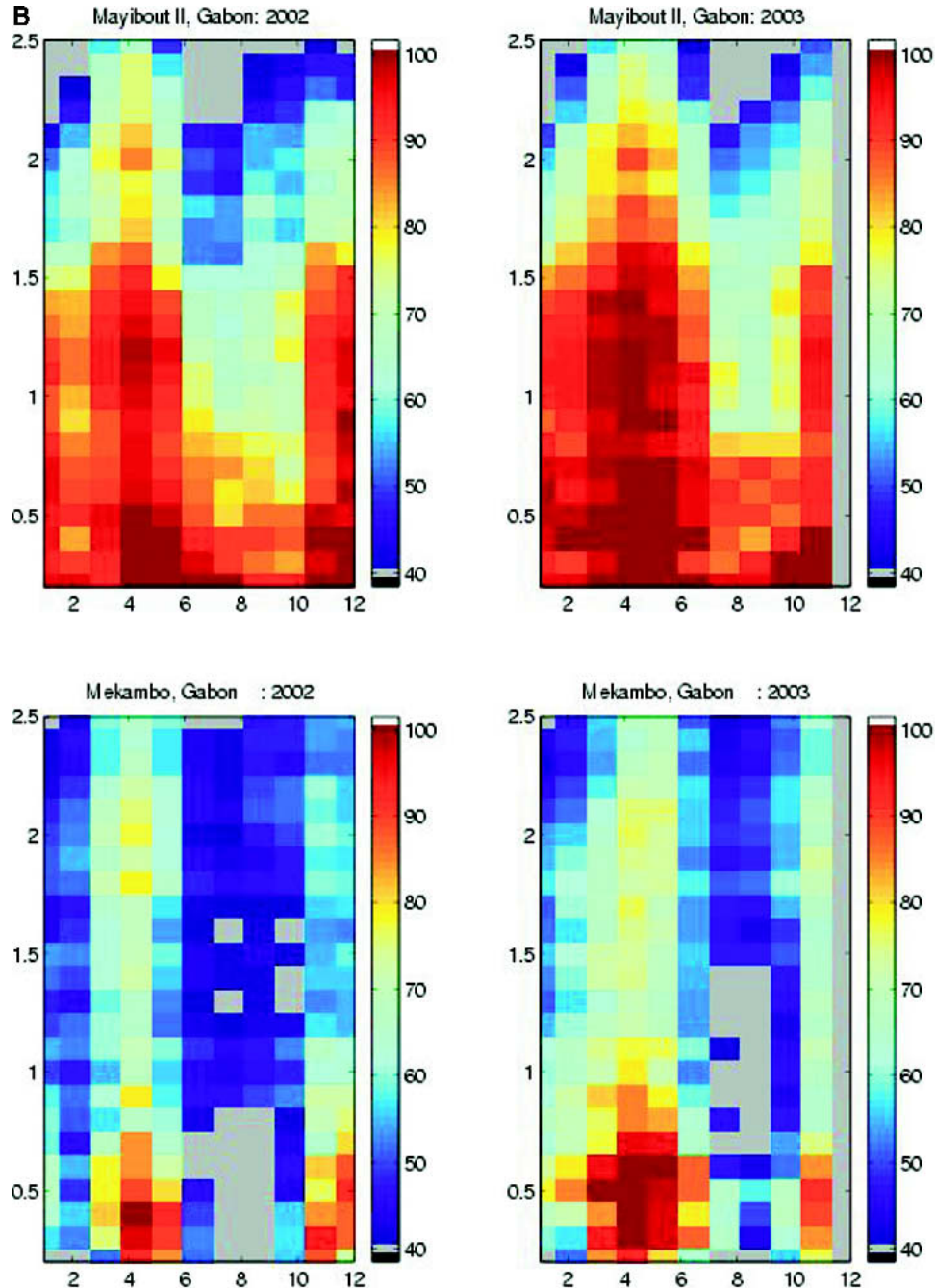


FIGURE 3. (Continued) Geotemporal distribution of pixels exhibiting negative anomalies during the months before the outbreak. Distance from the location of the sites where the Ebola outbreaks were reported (in degrees) is represented by the y-axis. Months from January to December of the outbreak year are represented on the x-axis. The color convention represents the percentage of pixels in the region with negative anomalies (as represented by red pixels). One degree equals approximately 110 km. DRC = Democratic Republic of Congo. This figure appears in color at www.ajtmh.org.

km (2.5 geographic degrees) from the site during the year of the outbreak. The Tai (1994), Mekouka (1994), and Mekambo (2001) Ebola outbreaks were associated with negative anomalies two months before the first case of Ebola. These large anomalies occurred during the second rainy season of the year. Of interest is the unique high risk characteristic of negative anomalies in the Mekouka site during the whole year. The 1996 outbreaks in Gabon are preceded by short and localized negative anomalies, suggesting ongoing transmission from a prior time period.

The outbreak of Kéllé (2002–2003) in the Republic of Congo had two particular properties: 1) two separate months with negative anomalies; and 2) the center of the negative anomalies occurred distant (by 0.85 degrees) from the outbreak site, supporting the observation of outbreak extension from nearby sites (Mekambo and Mayibout II, Gabon, Figure 3B). The Kikwit and Gulu outbreaks (both with unimodal rainy seasons) occurred after a negative anomaly appeared in areas at least 140 km (1.3 degrees) from the site or at least four months before the first case of Ebola. We hypothesize the temporal delay between negative anomaly and first appearance of Ebola in humans may be explained by undetected transmission in non-human primates as described previously.¹⁶

We found several important criteria for definition of an Ebola trigger event. Table 2 shows the number of pixels (highlighted) associated with a high EGT2 index for all of Africa for each year (Np); the average of minimum distance to Ebola sites (D); the overall transmission trigger index (R); the percentage of Np associated with each individual Ebola site (% of Np); and the minimum/mode distances from a trigger event to an Ebola site (d). Notice the high concentration of anomalous grid points around Gabon sites (50% with minimum distance of 2 km and mode distance less than 100 km). The repeated occurrences of environmental stress conditions in this region are a warning of possible future outbreaks of this enigmatic disease. Figure 4 shows the transmission risk R values in Table 2 obtained from the results of the CCA in the spatial domain for each year. For display purposes the R values less than 2.75 were rescaled by one-third. Note that Figure 4 shows 1994 as a year of a significant trigger event that spanned Côte d'Ivoire, Gabon, and the Democratic

Republic of Congo. Years highlighted with no associated appearance of Ebola, such as 1989, were associated with a low overall transmission risk index (< 3.5), indicating low environmental transmission competency potential. The year 1991 was the year with maximum number of pixels and trigger index highlighted. This was due to the general disruption in recorded NDVI over global tropical forest after the eruption of Mount Pinatubo.^{42,43}

Figure 5 shows map risk indices for Africa by year based on the EGT2 index to produce a geotemporal composite risk for all of Africa. We propose that trigger index values greater than 2.75 indicate increased risk of environmental transmission of Ebola virus.

DISCUSSION

Table 2 highlights 1994 and 2003 as years of highest overall trigger index (R = 7.26 and R = 7.51, respectively). When comparing their distances (D), however, the proximity to an Ebola site is closer in 1994 than 2003. Moreover, there are more pixels involved in their trigger event, especially in Gabon, where the concentration of these points is higher (mode distance = 71). Several other Ebola outbreaks were highlighted such as those in 2000 and 2001. In 1989, a relative low R value was noted with an associated close proximity (d) to Gabon sites; however, no Ebola outbreaks were reported in Africa during this time. This may relate to non-human cases occurring undetected. In contrast, the reported cases of Ebola in 1996 were associated with a trigger index value less than four and the lowest percent of pixels near Ebola sites in Gabon. We interpret this as a residual Ebola presence in the environment from the 1994 period.

We recognized the possibility of introducing errors into our analysis due to 1) the hypothesis that Ebola can be transmitted among non-human primate species, 2) the difficulty in determining a primary Ebola outbreak from a secondary or tertiary one; and 3) undetected cases likely occurring. Lastly, the emergence of Ebola virus might not involve primates but other animals such as bats or rats. Nevertheless, we found two time periods during the past 23 years when trigger events were present in equatorial Africa and no Ebola outbreaks were reported (i.e., 1989, 1991; Figures 4 and 5). We interpret

TABLE 2

Geo temporal trigger indices for all of Africa and Ebola outbreak sites with trigger index components: number of pixels involved (Np), mean value of the distance from involved pixels to Ebola site (D, kilometers), overall trigger index (R), percentage of Np associated with each individual Ebola site (% Np), and minimum/mode distance, in kilometers, from a trigger event to an Ebola site (d)*

| Years | Np | D | R | Côte d'Ivoire | | DRC | | Uganda | | Gabon | |
|-----------|-------|------|------|---------------|--------|------|--------|--------|--------|-------|-------|
| | | | | % Np | D | % Np | d | % Np | d | % Np | d |
| 1982–1988 | 2,618 | 7.8 | 2.15 | | | | | | | | |
| 1989 | 3,406 | 10.4 | 3.09 | 4 | 17/197 | 22 | 17/186 | 17 | 6/123 | 56 | 2/68 |
| 1990 | 3,522 | 6.4 | 2.56 | | | | | | | | |
| 1991 | 6,406 | 2.6 | 7.7 | 13 | 3/194 | 23 | 1/194 | 17 | 3/115 | 47 | 2/76 |
| 1992–1993 | 2,674 | 7.6 | 2.13 | | | | | | | | |
| 1994 | 6,151 | 3.2 | 7.26 | 19 | 3/187 | 28 | 1/196 | 3 | 6/121 | 50 | 2/71 |
| 1995 | 2,452 | 8.7 | 2.11 | | | | | | | | |
| 1996 | 4,247 | 5.6 | 3.53 | 14 | 6/193 | 23 | 11/195 | 19 | 3/107 | 44 | 2/66 |
| 1997–1999 | 2,921 | 8.5 | 1.39 | | | | | | | | |
| 2000 | 4,478 | 4.8 | 4.53 | 18 | 3/176 | 27 | 1/194 | 11 | 12/167 | 44 | 2/81 |
| 2001 | 4,648 | 4.5 | 5.64 | 21 | 3/162 | 18 | 7/198 | 13 | 6/165 | 47 | 2/83 |
| 2002 | 2,650 | 4.5 | 3.61 | 18 | 6/192 | 12 | 7/198 | 20 | 3/148 | 50 | 2/85 |
| 2003 | 4,733 | 4 | 7.51 | 12 | 6/193 | 17 | 7/147 | 22 | 3/155 | 50 | 2/133 |

* DRC = Democratic Republic of the Congo.

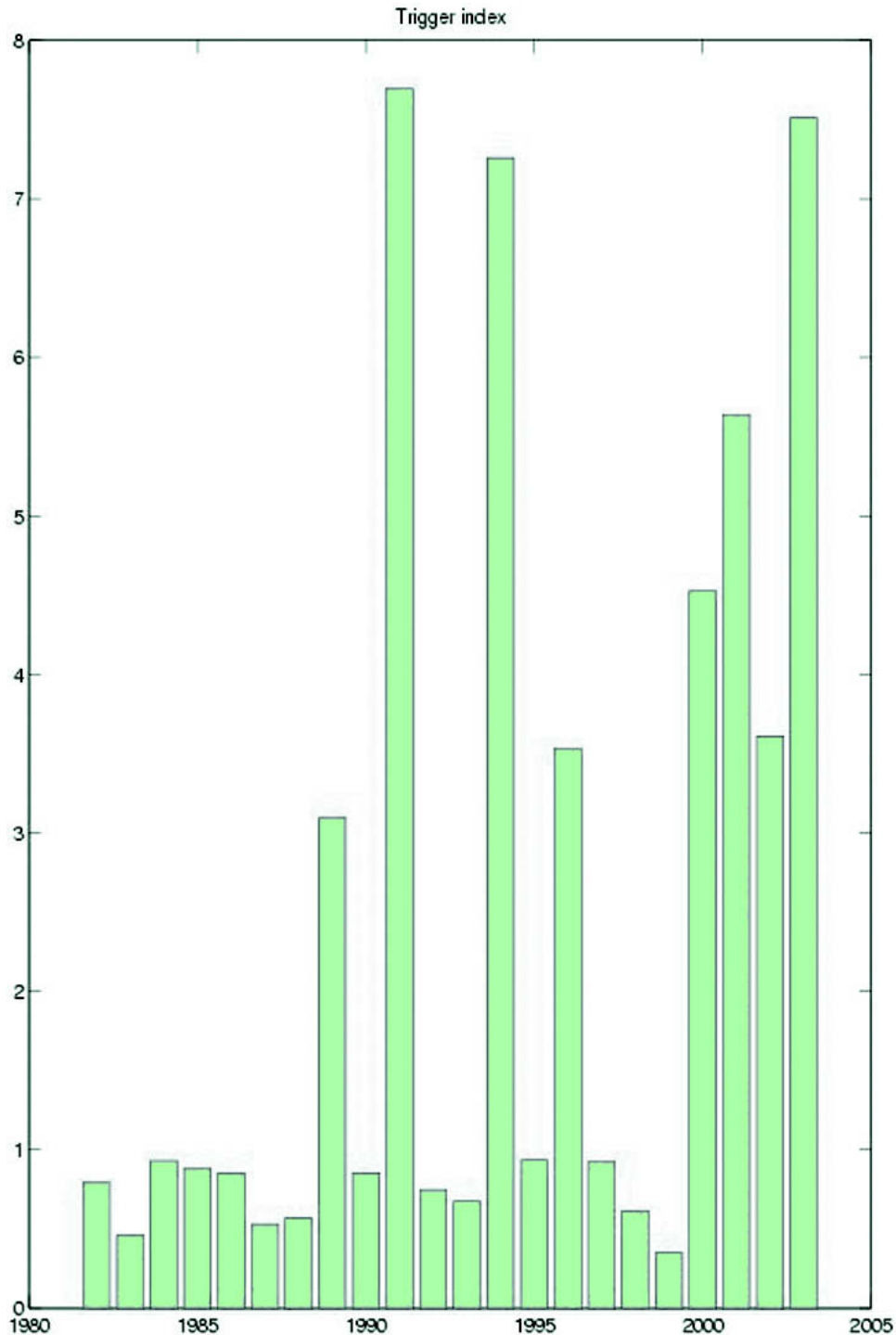


FIGURE 4. Ebola GeoTemporal Trigger Index showing the results of the Canonical Correlation Analysis in the spatial domain for each year for all known Ebola-endemic regions of Africa. This figure appears in color at www.ajtmh.org.

this to mean that either no transmission of the Ebola virus occurred in non-human primates and humans or an unidentified epidemic may have occurred at that time.

It has been previously suggested the consistent appearance of Ebola during the rainy season may be related to increased numbers of insects and mammals.⁶ Insect biomass in Makokou, Gabon has been reported to be 3.9 times greater during the rainy season from mid-October to mid-December.⁴⁴

Dramatic seasonal changes in fruiting and foraging behavior in primates, squirrels, and birds have been documented in Côte d'Ivoire and Gabon, where diet overlap and competition for the same food source has been observed during the period of maximum fruit production during the rainy season.^{6,44-47} The trigger event described in this study, beyond the seasonal enviroclimatic influences on Ebola transmission, may provide an added influence that results in greater contact of candidate

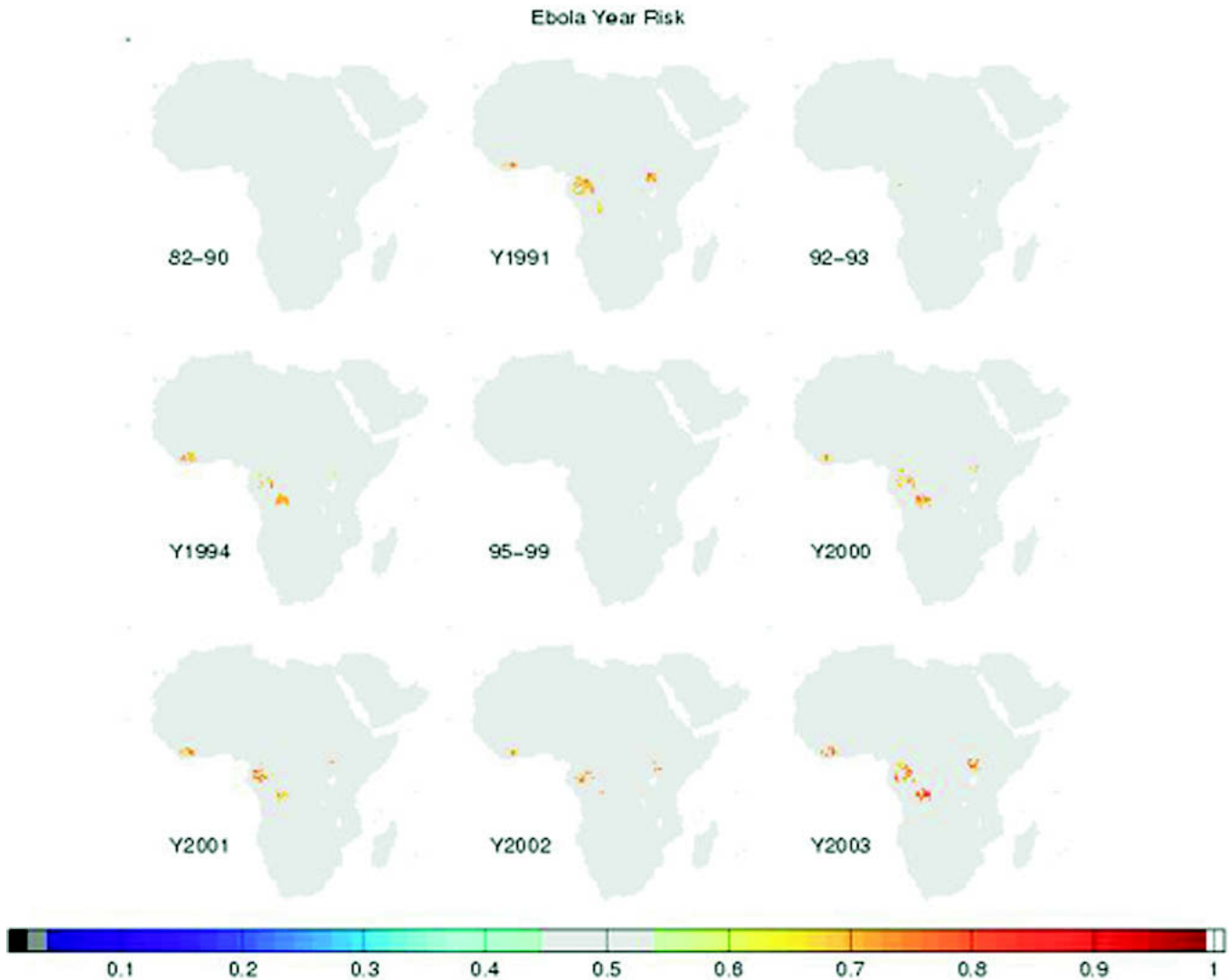


FIGURE 5. Yearly Canonical Correlation Analysis risk map of regions with characteristics of a trigger event according to the Ebola Geo-Temporal Trigger (EGT2) Index. This figure appears in color at www.ajtmh.org.

host insect and animals that become exposed to the cryptic Ebola reservoir through changes in foraging behavior.

The findings of this investigation suggest that highlighting conditions favorable for Ebola virus transmission is critical information for health care workers in Côte d'Ivoire, the Republic of Congo, the Democratic Republic of Congo, Uganda, and Gabon. We will continue our analysis and publicize our predictions to enable confirmation or refutation of our predictions. We have mapped the areas of potential Ebola outbreaks based on the time series analysis for the unimodal and bimodal rainy season locations shown in Figure 1. If our analysis is correct, future Ebola outbreaks will only occur in these areas and not elsewhere in equatorial Africa (Figure 5).

Received February 9, 2004. Accepted for publication April 24, 2004.

Acknowledgments: We thank Brian Rothman (University of Cincinnati College of Medicine), Neal Woolen (United States Army Medical Research Institute of Infectious Diseases), David Heymann, Guénael Rodier (World Health Organization Communicable Diseases Cluster), Richard Hatchett (United States Department of Health and Human Services), and Dr. Robert Vanessea for their valuable assistance.

Financial support: The appointments of James M. Wilson to the World Health Organization Ebola Tai Forest Project and the NASA-Goddard Space Flight Center were supported jointly by the Department of Communicable Diseases Surveillance and Response, the World Health Organization, and the Office of Applications, NASA.

Authors' addresses: Jorge E. Pinzon, Biospheric Sciences Branch, Laboratory for Terrestrial Physics, Code 923, National Aeronautics and Space Administration-Goddard Space Flight Center, Greenbelt, MD 20771 and Science Systems & Applications, Inc., Lanham, MD 20706, Telephone: 301-614-6685, Fax: 301-614-6015, E-mail: pinzon@negev.gsfc.nasa.gov. James M. Wilson, Global Alert and Response Team, Department of Communicable Diseases Surveillance and Response, World Health Organization, Geneva, Switzerland, E-mail: wilson@isis.imac.georgetown.edu. Compton J. Tucker, Sciences Branch, Laboratory for Terrestrial Physics, Code 923, National Aeronautics and Space Administration-Goddard Space Flight Center, Greenbelt, MD 20771, E-mail: compton@kratmos.gsfc.nasa.gov. Ray Arthur and Pierre Formenty, Global Alert and Response Team, Department of Communicable Diseases Surveillance and Response, World Health Organization, Geneva, Switzerland, E-mails: rca8@cdc.gov and formenty@who.int. Peter B. Jahrling, U.S. Army Medical Research Institute for Infectious Disease, Fort Detrick, Frederick, MD 21702-5011, E-mail: Peter.Jahrling@det.amedd.army.mil.

Reprint requests: Jorge E. Pinzon, Laboratory for Terrestrial Physics, Code 923, NASA/Goddard Space Flight Center, Greenbelt, MD 20771, Telephone: 301-614-6685, Fax: 301-614-6015, E-mail: pinzon@negev.gsfc.nasa.gov.

REFERENCES

- Peters CJ, LeDuc JW, 1999. An introduction to Ebola: the virus and the disease. *J Infect Dis* 179: 9–16.
- World Health Organization, 1976. Ebola hemorrhagic fever in Sudan, 1976. *Bull World Health Organ* 56: 247–270.
- World Health Organization, 1976. Ebola hemorrhagic fever in Zaire, 1976. *Bull World Health Organ* 56: 271–293.
- Heymann DL, Weisfeld JS, Webb PA, Johnson KM, Cairns T, Berquist H, 1980. Ebola hemorrhagic fever: Tandala, Zaire, 1977–1978. *J Infect Dis* 142: 372–376.
- Baron RC, McCormick JB, Zubeir OA, 1983. Ebola virus disease in southern Sudan: hospital dissemination and intrafamilial spread. *Bull World Health Organ* 61: 997–1003.
- Formenty P, Boesch C, Wyers M, Steiner C, Donati F, Dind F, Walker F, Le Guenno B, 1999. Ebola virus outbreak among wild chimpanzees living in a rain forest of Côte d'Ivoire. *J Infect Dis* 179: S120–S126.
- Formenty P, Hatz C, LeGuenno B, Stoll A, Rogenmoser P, Widmer A, 1999. Human infection due to Ebola virus, subtype Côte d'Ivoire: clinical and biologic presentation. *J Infect Dis* 179: S48–S53.
- Amblard J, Obiang P, Prechaud C, Bouloy M, LeGuenno B, 1997. Identification of the Ebola virus in Gabon in 1994. *Lancet* 349: 181–182.
- Georges AJ, Leroy EM, Renaut AA, Benissan CT, Nabias RJ, Ngoc MT, Obiang PI, Lepage JP, Bertherat EJ, Benoni DD, Wickings EJ, Amblard JP, Lansoud-Soukate JM, Milleliri JM, Baize S, Georges-Courbot MC, 1999. Ebola hemorrhagic fever outbreaks in Gabon, 1994–1997: epidemiologic and health control issues. *J Infect Dis* 179: S65–S75.
- Muyembe-Tamfum JJ, Kipasa M, 1995. Ebola hemorrhagic fever in Kikwit, Zaire. *Lancet* 345: 1448.
- Centers for Disease Control and Prevention, 2001. Outbreak of Ebola hemorrhagic fever-Uganda, August 2000-January 2001. *MMWR Morb Mortal Wkly Rep* 50: 73–77.
- World Health Organization, 2001. Outbreak of Ebola haemorrhagic fever, Uganda, August 2000-January 2001. *Wkly Epidemiol Rec* 76: 41–46.
- World Health Organization, 2003. Outbreak(s) of Ebola haemorrhagic fever, Congo and Gabon, October 2001–July 2002. *Wkly Epidemiol Rec* 78: 217–224.
- Leroy EM, Rouquet P, Formenty P, Souquière S, Kilbourne A, Froment J-M, Bermejo M, Smit S, Karesh W, Swanepoel R, Zaki SR, Rollin PE, 2004. Multiple Ebola virus transmission events and rapid decline of Central African wildlife. *Science* 303: 387–390.
- World Health Organization, 2003. Outbreak(s) of Ebola haemorrhagic fever in the Republic of Congo, January–April 2003. *Wkly Epidemiol Rec* 78: 285–296.
- Walsh PD, Abernethy KA, Bermejo M, Beyers R, de Wachter P, Akou ME, Huijbregts B, Mambounga DI, Toham AK, Kilbourn AM, Lahm SA, Latour S, Maisels F, Mbina C, Mihindou Y, Obiang SN, Effa EN, Starkey MP, Telfer P, Thibault M, Tutin CE, White LJ, Wilkie DS, 2003. Catastrophic ape decline in western equatorial Africa. *Nature* 422: 611–614.
- Arata AA, Johnson B, 1978. Approaches towards studies on potential reservoir of viral haemorrhagic fever in southern Sudan (1977). Pattyn SR, ed. *Ebola Virus Haemorrhagic Fever*. Proceedings of an International Colloquium on Ebola Virus Infection and Other Haemorrhagic Fevers. Antwerp, Belgium, December 6–8, 1977. Amsterdam: Elsevier/North-Holland Biomedical Press, 191–202.
- Germain M, 1978. Collection of mammals and arthropods during the epidemic of haemorrhagic fever in Zaie. Pattyn SR, ed. *Ebola Virus Haemorrhagic Fever*. Proceedings of an International Colloquium on Ebola Virus Infection and Other Haemorrhagic Fevers. Antwerp, Belgium, December 6–8, 1977. Amsterdam: Elsevier/North-Holland Biomedical Press, 185–189.
- Reiter P, Turell M, Coleman R, Miller B, Maupin G, Liz J, Kuehne A, Barth J, Geisbert J, Dohm D, Glick J, Pecor J, Robbins R, Jahrling P, Peters C, Ksiazek T, 1999. Field investigations of an outbreak of Ebola Hemorrhagic fever, Kikwit, Democratic Republic of the Congo: arthropod studies. *J Infect Dis* 179: S148–S154.
- Leirs H, Mills JN, Krebs JW, Childs JE, Akaibe D, Woollen N, Ludwig G, Peters CJ, Ksiazek TG, 1999. Search for the Ebola virus reservoir in Kikwit, Democratic Republic of the Congo: reflections on a vertebrate collection. *J Infect Dis* 179: S155–S163.
- Breman JG, Johnson KM, van der Groen G, Robbins CB, Szczeniowski MV, Ruti K, Webb PA, Meier F, Heymann DL, 1999. A search for Ebola virus in animals in the Democratic Republic of the Congo and Cameroon: ecologic, virologic, and serologic surveys, 1979–1980. *J Infect Dis* 179: S139–S147.
- Johnson BK, Wambui C, Ocheng D, Gichogo A, Oogo S, Libondo D, Gitau LG, Tukei PM, Johnson ED, 1986. Seasonal variation in antibodies against Ebola virus in Kenyan fever patients (letter). *Lancet* 8490: 1160.
- Monath TP, 1999. Ecology of Marburg and Ebola viruses: speculations and directions for future research. *J Infect Dis* 179: S127–S138.
- Tucker CJ, Wilson JM, Mahoney R, Anyamba A, Linthicum K, Myers MF, 2002. Climatic and ecological context of the 1994–1996 Ebola outbreaks. *Photogrammetric Eng Remote Sens* 68: 174–152.
- Wilson JM, Tucker CJ, 2002. Use of remote sensing in epidemic surveillance and response. *World Meteorol Organ Bull* 51: 136–139.
- Cracknell, AP, 1997. *The Advanced Very High Resolution Radiometer*. London: Taylor and Francis, 534.
- Kidwell KB, 1997. *NOAA Polar Orbiter Users Guide*. Rockville, MD: National Oceanic and Atmospheric Administration.
- Pinzon JE, Brown ME, Tucker CJ, 2004. Satellite time series correction of orbital drift artifacts using empirical mode decomposition. Huang NE, Shen SSP, eds. *EMD and Its Applications*. Singapore: World Scientific 10: 285–295.
- Pinzon JE, 2002. Using HHT to successfully uncouple seasonal and interannual components in remotely sensed data. *SCI 2002 Proceedings*. Orlando, FL, July 14–18, 2002.
- Lotsch A, Friedl MA, Pinzon JE, 2003. Spatio-temporal deconvolution of NDVI image sequences using independent component analysis. *IEEE Trans Geosci Remote Sens* 41: 2938–2942.
- Tucker CJ, 1979. Red and photographic infrared linear combinations for monitoring vegetation. *Remote Sens Environ* 8: 127–150.
- Myneni RB, Hall FG, Sellers PJ, Marshak AL, 1995. The interpretation of spectral vegetation indexes. *IEEE Trans Geosci Remote Sensing* 33: 481–486.
- Tucker CJ, Sellers PJ, 1986. Satellite remote sensing of primary production. *Int J Remote Sens* 7: 1395–1416.
- Justice CO, Holben BN, Gwynne MD, 1986. Monitoring East African vegetation using AVHRR data. *Int J Remote Sens* 7: 1453–1474.
- Nicholson SE, Davenport ML, Malo AR, 1990. A comparison of vegetation response to rainfall in the Sahel and east Africa using Normalized Difference Vegetation Index from NOAA-AVHRR. *Climate Change* 17: 209–241.
- Cihlar J, St. Laurent L, Dyer JA, 1991. The relation between Normalized Difference Vegetation Index and ecological variables. *Remote Sens Environ* 35: 279–298.
- Linthicum KJ, Anyamba A, Tucker CJ, Kelley PW, Myers MF, Peters CJ, 1999. Climate and satellite indicators to forecast Rift Valley fever epidemics in Kenya. *Science* 285: 397–400.
- Linthicum KJ, Bailey CL, Davies FG, Tucker CJ, 1987. Detection of Rift Valley fever viral activity in Kenya by satellite remote sensing imagery. *Science* 235: 1656–1659.
- Betherton CS, Smith C, Wallace JM, 1992. An intercomparison of methods for finding coupled patterns in climate data. *J Climate* 5: 541–560.
- Wallace JM, Smith C, Betherton CS, 1992. Singular value decomposition of winter time sea surface temperature and 500-mb height anomalies. *J Climate* 5: 561–576.
- Cherry S, 1996. Singular value decomposition analysis and canonical correlation analysis. *J Climate* 9: 2003–2009.

42. Vermote EF, El Saleous NZ, Kaufman YF, Dutton E, 1997. Data pre-processing: stratospheric aerosol perturbing effect on the remote sensing of vegetation: correction method for the composite NDVI after the Pinatubo eruption. *Remote Sens Rev* 15: 7–21.
43. Hansen J, Lacis A, Ruedy R, Sato M, 1992. Potential climate impact of Mount Pinatubo eruption. *Geophys Res Lett* 19: 215–218.
44. Wright SJ, 1996. Phenological responses to seasonality in tropical forest plants. Mulkey SS, Chazdon RL, Smith AP, eds. *Tropical Forest Plant Ecophysiology*. New York: Chapman & Hall/International Thomson Publishing Company, 450–455.
45. Emmons LH, 1980. Ecology and resource partitioning among nine species of African rain forest squirrels. *Ecol Monogr* 50: 31–54.
46. Gautier-Hion A, 1980. Seasonal variations of diet related to species and sex in a community of *Cercopithecus* monkeys. *J Anim Ecol* 49: 237–269.
47. Gautier-Hion A, Michaloud G, 1989. Are figs always keystone resources for tropical frugivorous vertebrates? A test in Gabon. *Ecology* 70: 1826–1833.